PCCP

Accepted Manuscript

ROYAL SOCIETY OF CHEMISTRY

www.rsc.org/pccp

Regular arrays of Pd and PdAu clusters on ultrathin alumina films for reactivity studies.

M. Marsault, G. Sitja, C.R. Henry*

Centre Interdisciplinaire de Nanoscience de Marseille, Aix-Marseille Université/CNRS, UMR 7325, Campus de Luminy, Case 913, F-13288 Marseille cedex 09, France

*Corresponding author, email :henry@cinam.univ-mrs.fr

Abstract

Hexagonal arrays of Pd and PdAu clusters are produced by condensation of metal vapors under UHV on a nanostructured alumina ultrathin film at 320 K. The alumina presents a hexagonal network of point defects that are nucleation centers for Pd. The growth of the Pd clusters is uniform leading to a very narrow size distribution in the range of size of few atoms to about 400 atoms. The number density of clusters is fixed by the density of nodes of the nanostructure of the alumina film ($6.5x10^{12}$ cm^{-2}). The PdAu bimetallic particles grow in a two-steps process. First Pd is deposited then Au is deposited and grows exclusively on the preformed Pd clusters. The size and the composition of the clusters are independently controlled by the amounts of the deposited metals. The shape, size, density and organization of the clusters are studied in situ by STM. The long range order is studied in situ by Grazing Incidence Small Angle X-ray Scattering (GISAXS). The organization of the arrays of clusters is stable up to 600 K. These arrays of Pd and PdAu clusters on alumina are well suited model catalysts to study the effects of size, shape and composition on their reactivity.

I. Introduction

To understand the basic mechanisms in heterogeneous catalysis it is necessary to work on supported model catalysts because real catalysts are very difficult to characterize at the atomic scale. Supported model catalysts are generally obtained by growing under UHV metal nanoparticles on oxide flat supports that can be characterized in detail by surface science tools [1-4]. These studies have shown that for a given catalytic metal the reactivity depends on the size, of the shape of the nanoparticles but also on their spatial distribution and on the nature of the oxide support [5]. Ideally it is necessary to control independently all these parameters. In practice, the metal clusters are randomly distributed on the support with a size dispersion which in rather broad, in the best case it can be 25% of the mean size [2]. This is due to the fact that metal clusters nucleate on the defects of the oxide substrate which are randomly distributed [6]. One way to have lower size dispersion is to prepare clusters in a free beam to size select them and to deposit them on the substrate. If the kinetic energy of the deposited clusters is low (soft-landing) the deposited clusters remain intact [7]. Now it is possible to deposit size selected clusters of any kind of metal from single atom to about 5000 atoms [8-12], however the distribution of the clusters is random. A way to prepare clusters regularly distributed on a substrate with a narrow size distribution is to grow them by deposition of atoms on a template which is composed by a regular network of defects. The first templates used to grow arrays of clusters were based on a dislocation network generated by the misfit between a thin layer

of metal and a metallic substrate [13]. Later on, surface reconstruction of Au vicinal surfaces [14] or chemisorbed nitrogen monolayer on a Cu [15] have been used. However for model catalysis an inert support is required. Only recently an oxide template to grow regular arrays of metal clusters of Ag and Mn has been discovered; it is an ultrathin (0.5 nm thick) alumina film obtained by high temperature oxidation of a Ni_3Al (111) substrate [16]. This film has a band gap and a phonon spectrum close to those of bulk alumina but it is sufficiently thin to perform STM observation [17]. Depending of the bias voltage applied during STM observation two hexagonal superstructures appear with a lattice parameter of 4.1 nm ('dot' structure) or 2.4 nm ('network' structure) [16]. These superstructures do not correspond to a pure electronic effect because they are also observed by non-contact AFM [18, 19]. These AFM observations have shown that the surface of the film is composed of a hexagonal lattice of 0.29 nm with a very weak corrugation. Very high quality atomic resolution images of this film have been later obtained by STM [20]. From the comparison between STM images and DFT calculation a structural model has been proposed where the nodes of the dot structure are atomic holes in the top oxygen layer of the alumina film [20]. This template has been used to grow at RT arrays of Cu [21], Ag [16], Au [22, 23], Pd [24, 25, 20, 26], Fe [27, 28], Co [28], Mn [16], V [21]. Noble metals (Cu, Ag, Au, Pd) nucleate at the nodes of the dot structure to form an array of clusters separated by 4.1 nm. However, only Pd forms a very regular array at high coverage. On the contrary transition metals have a tendency to nucleate on the network structure but only vanadium forms a highly ordered array with a parameter of 2.4 nm. For Co, Fe and Mn disorder appears well before that all the sites of the network structure are occupied. We have shown that by depositing Au on an array Pd clusters gold atoms grow only on the previously formed Pd clusters resulting in a perfect array of bimetallic PdAu nanoparticles [25]. The clear advantage of this method of fabrication of bimetallic clusters is that the size and the chemical composition of the clusters are independently controlled by the total amount of atoms deposited and by the ratio of the amounts of the two types of atoms, respectively [29]. The use of an array of Pd clusters as seed (few atoms of Pd are enough) to grow regular arrays of Fe [20, 28], Co [28] and Ni clusters [30]. The use of pre-nucleated clusters (Co) as seeds for the deposition of a second metal (Pd) has been previously reported in the growth of PdCo clusters on alumina ultrathin films on NiAl (110) [31]. However the fact that the Co clusters were randomly distributed (unlike on Ni_3Al (111) the alumina film on NiAl (110) does not present a regular nanostructure) led to size and composition distributions much larger than by using a regular array of clusters [29].

The long range order of Pd [26, 28], PdAu [32] arrays has been studied grazing incidence small angle X-ray scattering (GISAXS [33]). Both types of clusters are well ordered on the whole sample but at high coverages disorder appears due to coalescence of clusters.

Pd arrays on the nanostructured alumina ultrathin film has been used as model catalysts to study the adsorption of CO molecules as a function of the size of the Pd clusters, from 5 atoms to a diameter of 6 nm [26]. This large range has allowed the observation of the transition between the non-scalable regime for which the reactivity depends on the number atoms in the cluster and the scalable regime for which the reactivity evolves monotonously with cluster size [26]. However to use regular arrays of clusters as model catalysts it is necessary to be sure that they are stable in the condition of the reaction (temperature, gas environment…). Recently new templates have been used to grow at RT regular arrays of metal clusters (Pt, Ni, Ir, Rh, Co) like graphene layer grown on a metallic substrate [34-38] or monolayer of BN on a metal surface [39] but the organization was not stable at a

temperature higher than 400 K and CO adsorption induces diffusion and coalescence of Pt clusters on graphene/Ir(111) [40].

In this paper we present a detailed study by STM and GISAXS of the growth and the organization of Pd and PdAu clusters on alumina ultrathin film on Ni_3Al (111) as a function the metal coverage and of the chemical composition in the case of PdAu . We present also the evolution of the organization of the clusters after annealing at a temperature up to 1000 K.

2. **Sample preparation**

The alumina ultrathin films are prepared following the method developed by C. Becker et al. [16] which consist to oxidize at high temperature a Ni_3Al (111) surface in a UHV chamber. The substrate is prepared by cycles of 30 minutes argon ion sputtering followed by annealing at 1100K during 15 min. The temperature of the sample surface is measured by a thermocouple which has been calibrated by an optical pyrometer. The oxidation of the substrate is made by exposition to an oxygen pressure of $5x10^{-8}$ mbar at 1000 K during 20 minutes. Then the sample is annealed at 1050 K for 7 min. Figure 1a displays a LEED pattern that is characteristic of the well-organized ultrathin oxide film. The nanostructuration of the alumina film is verified in situ by STM (OMICRON STM1) at RT. Figure 1b shows the dot structure (4.1 nm) and the network structures (2.4 nm) imaged by STM at bias voltages of 2.1 V and 3.2 V, respectively.

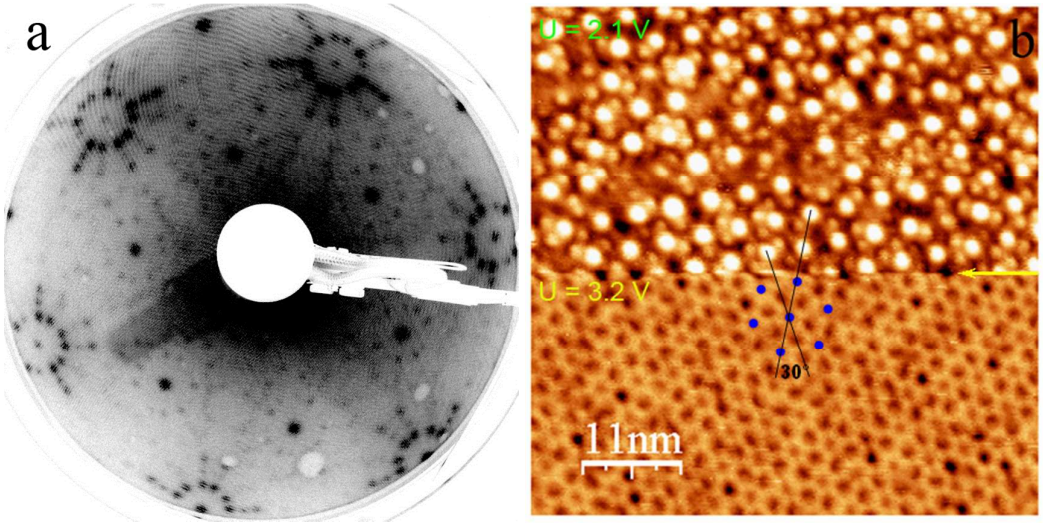

Figure 1: Alumina ultrathin film on Ni_3Al (111) substrate. LEED pattern (a) and STM image (b) obtained at bias voltages of 2.1 V (top) and 3.2 V (bottom).

The growth of Pd nanoparticles is made by depositing Pd atoms at 320 K from a Knudsen cell made of a graphite crucible heated by electron bombardment. The deposition rate is calibrated in situ by a quartz crystal microbalance. The deposition of Au is made by a second calibrated Knudsen cell. The condensation coefficient of both metals on the alumina is unity as determined by RBS (Rutherford

back-scattering) analysis of some samples. The arrays of PdAu nanoparticles are obtained by sequential depositions of known amounts of Pd (first) and Au (second) atoms at 320K.

The nanoparticles arrays are characterized in situ by STM (OMICRON STM1) at RT. The tungsten tips are prepared by a classical electrochemical etching procedure.

3. **Growth and stability of regular arrays of Pd nanoparticles**

Figure 2a displays an STM image of a 0.15 ML Pd deposit on the nanostructured alumina film. The image has been recorded at a voltage of 1.19 V for which the nanostructuration of the film is not visible; the hexagonal array of bright dots separated by 4.1 nm corresponds to the Pd clusters. Fig. 2b shows the Fourier transform of the image in (a) that shows that the Pd clusters are well organized and separated by 4.1 nm. In order to see where the Pd are sit, fig. 2c displays an STM image of a weak Pd deposit obtained at a bias voltage to 3.2 V for which it is possible to image simultaneously the Pd clusters (bright dots) and the network structure (dark spots) of the alumina film. We see clearly that the Pd clusters occupy exclusively the nodes of the dot structure.

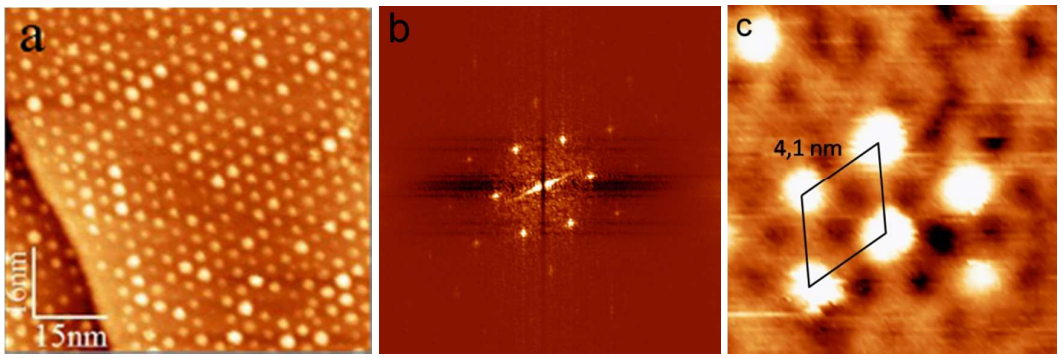

Figure 2: (a) STM image of 0.15 ML of Pd on the alumina film obtained a 1.19 V. (b) Fourier transform of the STM image on (a). (c) Image of a weak Pd deposit obtained at 3.2 V.

Figure 3 shows the nucleation kinetics of Pd clusters on the nanostructured alumina film at 320K. At a coverage of 0.025 ML about half of the nodes of the dot structure are occupied but rapidly the saturation of all the sites of the dot structure occurs. This behaviour is typical for nucleation of defects which here are the nodes of the dot structure [6]. At 1.5 ML the density of clusters decreases. At this coverage we do not expect growth-coalescence.

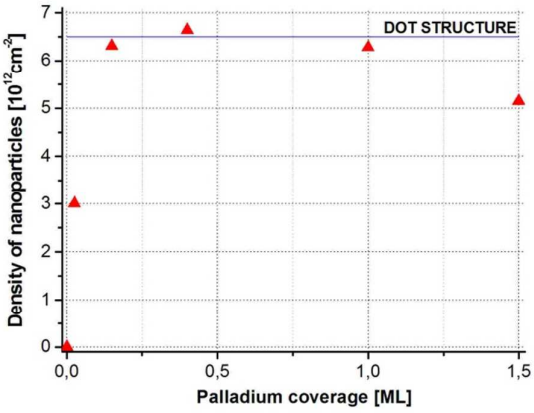

Figure 3: Number density of Pd clusters as a function of coverage at 320 K. The Pd flux is equal to $5x10^{12}$ atoms/s. cm^{-2}.

Figure 4 displays STM pictures of four Pd deposits (0.025, 0.15, 0.4 and 1.5 ML). For each deposit the clusters are well separated but at 1.5 ML the clusters seem to be less organized. This is confirmed by figure 5 which shows self-correlation images corresponding to 0.4 and 1.5 ML. At 1.5 Ml the clusters are no longer organized in a regular array. This can be explained by the fact that the clusters grow non-uniformly from the nucleation site. This hypothesis is supported by the fact that the size distribution is definitely broader at 1.5 ML and asymmetric. Growth coalescence is clearly visible at 10 ML where the density of clusters is reduced by 40% and the particles have very asymmetric shapes. Taking a hemispherical shape for the Pd particles static coalescence must occur at a coverage of 5 ML. The decrease of the density of clusters at 1.5 ML is probably due to the fact that large clusters are less trapped on the nodes of the dots structure and that they can move and coalesce with neighbouring clusters.

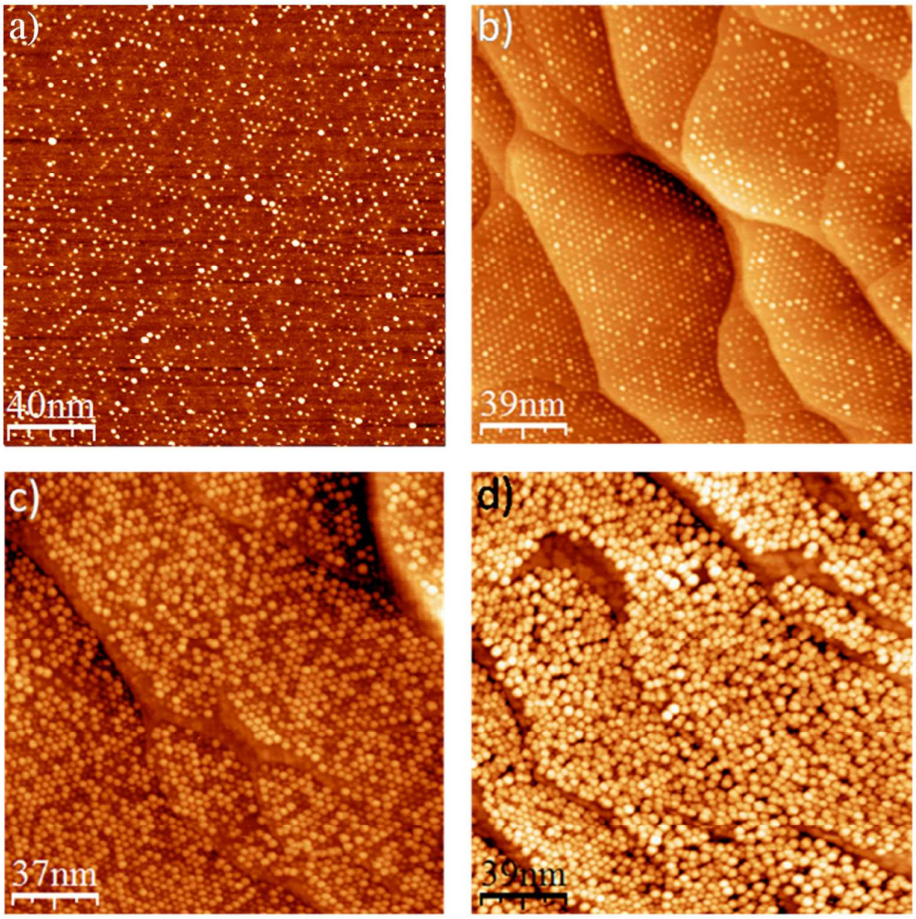

Figure 4: STM images (I_t = 19 pA, U= 1.19 V) of Pd deposit on alumina films on Ni_3Al (111): (a) 0.025 ML, (b) 0.15 ML, (c) 0.4 ML, (d) 1.5 ML. The mean sizes of the clusters are 6, 35, 94 and 352 atoms for images a, b, c and d, respectively.

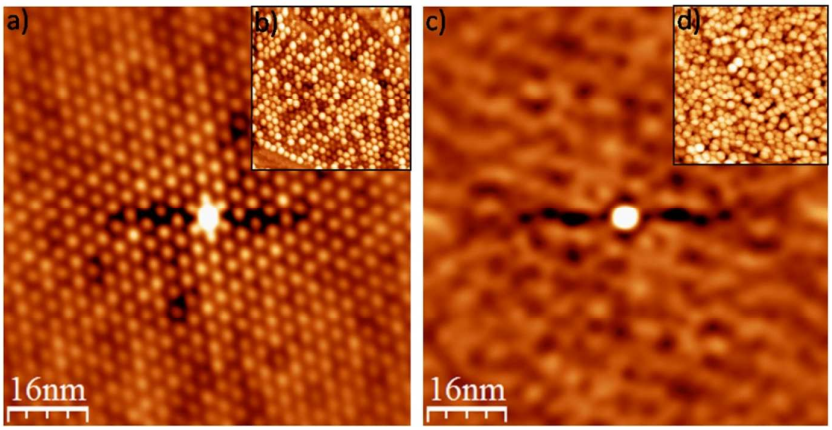

Figure 5: Self correlation images of STM pictures of Pd deposits corresponding to 0.4 ML (a) and 1.5 ML (c). The insets (b) and (d) represent corresponding STM pictures.

Figure 6 displays the size and the height distributions corresponding to a Pd deposit of 0.15 ML. The size measured by STM is larger than the true size of the clusters because of the finite dimension of

the STM tip. However the sharpness of the distribution ($\Delta D/D = 0.13$) is an indication that the actual size distribution is narrow. The height measured by STM is not affected by the tip shape but we know that it depends of the bias voltage [24, 28]. However the height distribution is non monotonous and shows peaks separated by roughly 0.2 nm that corresponds to successive Pd atomic layers.

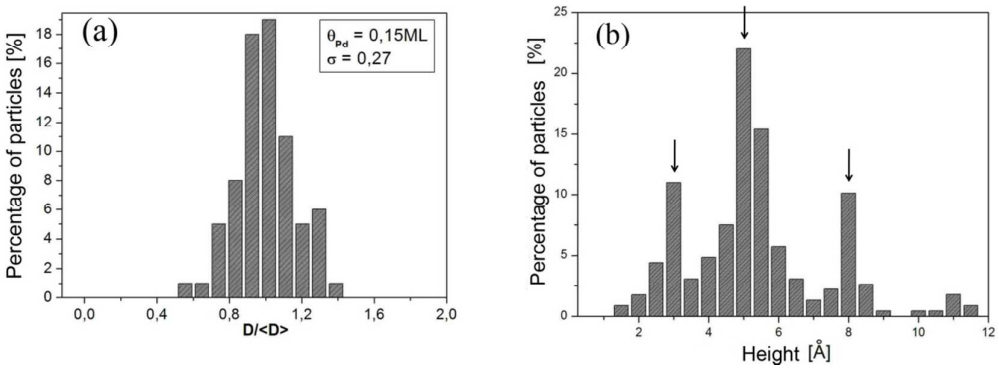

Figure 6: Size (a) and height distribution (b) of clusters from a 0.15 ML Pd deposit.

The thermal stability of the organization of the Pd arrays has been studied by annealing them under UHV at temperature step by step up to 1000 K. STM images of an array of Pd clusters with a mean size of 35 atoms (0.15 ML) after successive annealings are displayed on figure 7. The self-correlation images are represented in the insets.

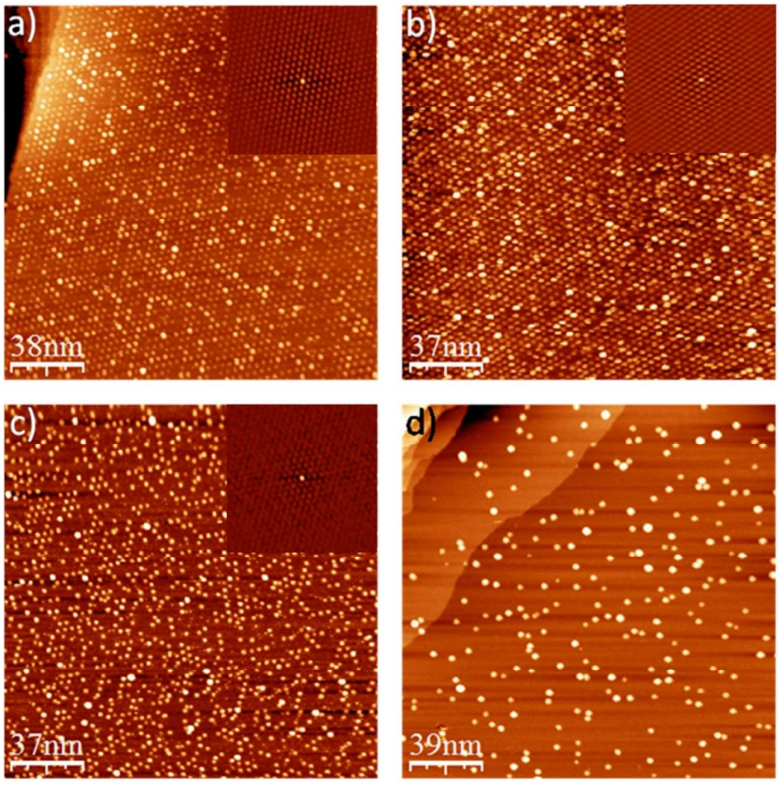

Figure 7: STM images (I_t = 19 pA, U = 1.49 V) of 0.15 Pd after annealing under UHV at 470K (a), 590 K (b), 670 K and 1000 K. Self-correlation images are displayed in inset for (a), (b) and (c) STM images.

Up to 590 K the organization of the Pd clusters is still perfect visually that is confirmed by the self-correlation images. At 670 K, a loss of order is clearly visible and at 1000K no order at all is visible on the image and the density of clusters is strongly reduced. The density of clusters as a function of annealing temperature is presented on figure 14. Up to 600K the density of clusters is constant and at higher temperature it decreased continuously. At 1000 K it is reduced by about 90%. What is at the origin of the loss of order in assembly of cluster and decrease of the density of clusters at high temperature? A first reason could be the migration of clusters followed by coalescence with other clusters. This assumption is justified by the fact that the size of the clusters and their height increase. But other mechanisms could also play a role like Ostwald ripening, evaporation or diffusion in the bulk through the alumina film. Ostwald ripening is not expected because at the origin the clusters are situated at equal distance and have a very low size dispersion. Concerning the desorption of Pd, it is known by temperature programmed desorption (TPD) that Pd does not desorbs from an oxide film at 1000K [41]. A recent paper reports that Pd atoms on the defects of the dot structure can diffuse through alumina ultrathin films at 570 K [28]. In order to check if some matter has disappeared from the surface of the films we have estimated the quantity of matter in the Pd clusters from the STM images. After deposition of 0.15 ML of Pd at 320 K the mean number of atoms per clusters is 35. The mean height is 0.64 nm from the distribution of height measured by STM (see fig 6b). We know that the particle size measured by STM is much larger than the actual value. However we can assume that the particles have the shape of a truncated sphere with a contact angle α. We find that α = 92 ° and an aspect ratio of 0.53. Previous STM measurements for Pd nanoparticles grown at RT on alumina ultrathin films on NiAl (110) have shown that the aspect ratio decreased from 0.35 to 0.15 when size increased (the smallest clusters having a size of about 3 nm) [42]. More recently for the same system a contact angle of 99° has been found for clusters of 1.21 nm in height [43]. After annealing at 1000 K the mean height is 1.17 nm and if one assumes no loss of matter α = 76° and the aspect ratio is 0.38. That would mean that the clusters are flatter. This could results from coalescence without restoration of the equilibrium shape. Otherwise one can assume that some of the matter is lost (for example by diffusion in the bulk). If we assume that the shape of the cluster is not changed (α = 92°), keeping the measured height (1.17 nm) the cluster diameter would be 2.4 nm that corresponds to a loss of matter of 33%. It is difficult to disentangle these two possibilities after annealing at 1000 K: flattening without loss of matter by diffusion in the bulk substrate or the shape is kept and some matter is lost; without accurate measurement of the actual diameter of the particles.

4. **Growth and stability of regular arrays of PdAu clusters**

We have already shown that the ultrathin alumina film on Ni_3Al (111) is not a good template to grow a regular array of Au clusters at RT [23]. This is probably due to the fact that at this temperature we are outside the window to have a perfect template which has been observed in Monte Carlo simulations [44]. This would mean that the sites of the dot structure are not perfect sinks for gold atoms at RT contrary to Pd atoms. Then the only way to grow regular arrays of PdAu clusters is to deposit successively Pd then Au as we have already shown [25]. Figure 8 shows an STM image of $Pd_{50}Au_{50}$ clusters obtained by condensing 0.15 ML of Pd followed by 0.15 ML of Au at 320K. The self-correlation image of the STM image shows clearly that the organization is very good (the bimetallic clusters are separated by 4.1 nm).

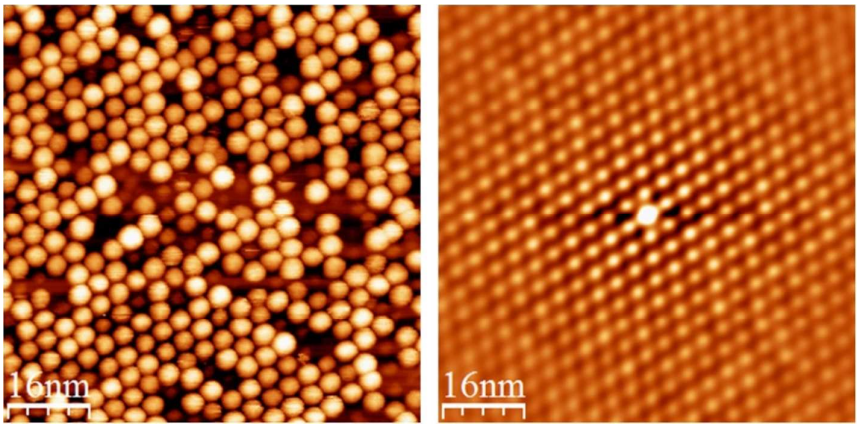

Figure 8: Array of PdAu clusters obtained by depositing successively 0.15 ML of Pd and 0.15 ML of Au at 320 K on the nanostructured alumina film. The mean size of the PdAu clusters is 70 atoms. On the left: STM image (I_t = 19 pA, U = 1.51 V); on the right: self- correlation image.

Figure 9 displays three STM images corresponding to an increase of Au content (Pd_3Au, PdAu and $PdAu_3$). The density of clusters is constant and equal to the density of the nodes of the dot structure. Visually the organization is very good that is confirmed by the Fourier transforms (see inset in the STM images).

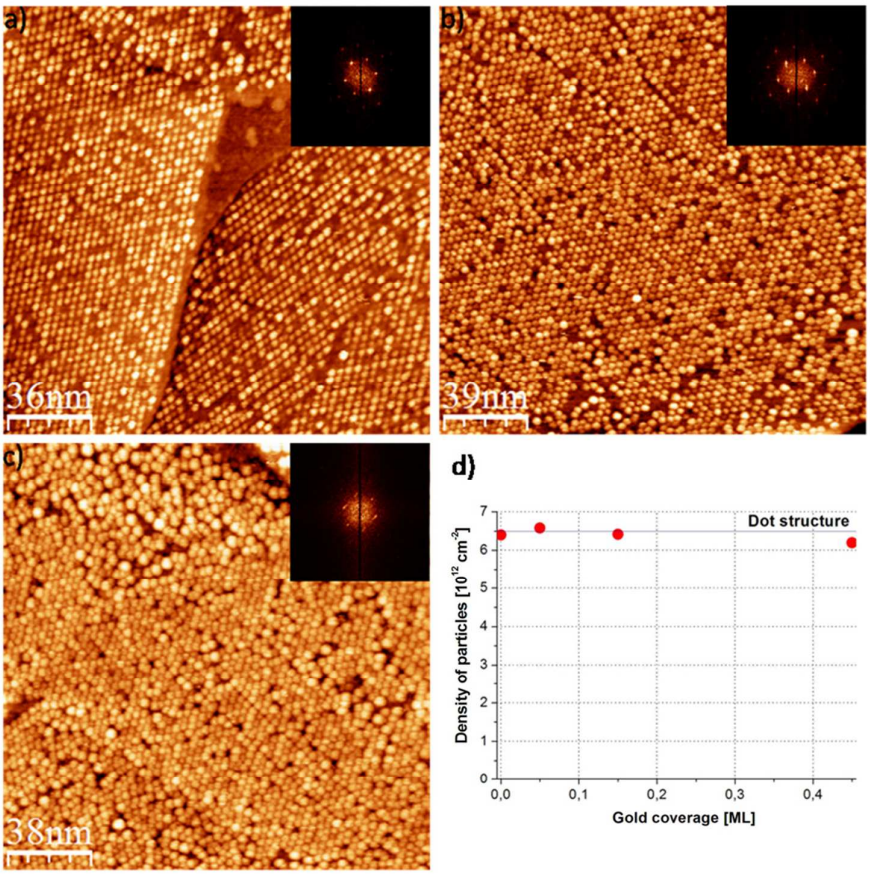

Figure 9: STM images (I_t = 19 pA, U = 1.51 V) corresponding to increasing amounts of Au deposited (a: 0.05 ML, b: 0.15 Ml, c: 0.45ML) on 0.15 ML of Pd. The insets are he Fourier transforms of the STM images. The density of clusters as a function of the amount of Au is plotted in (d). The mean size of the clusters is 47, 70, and 141 atoms for images (a), (b) and (c), respectively.

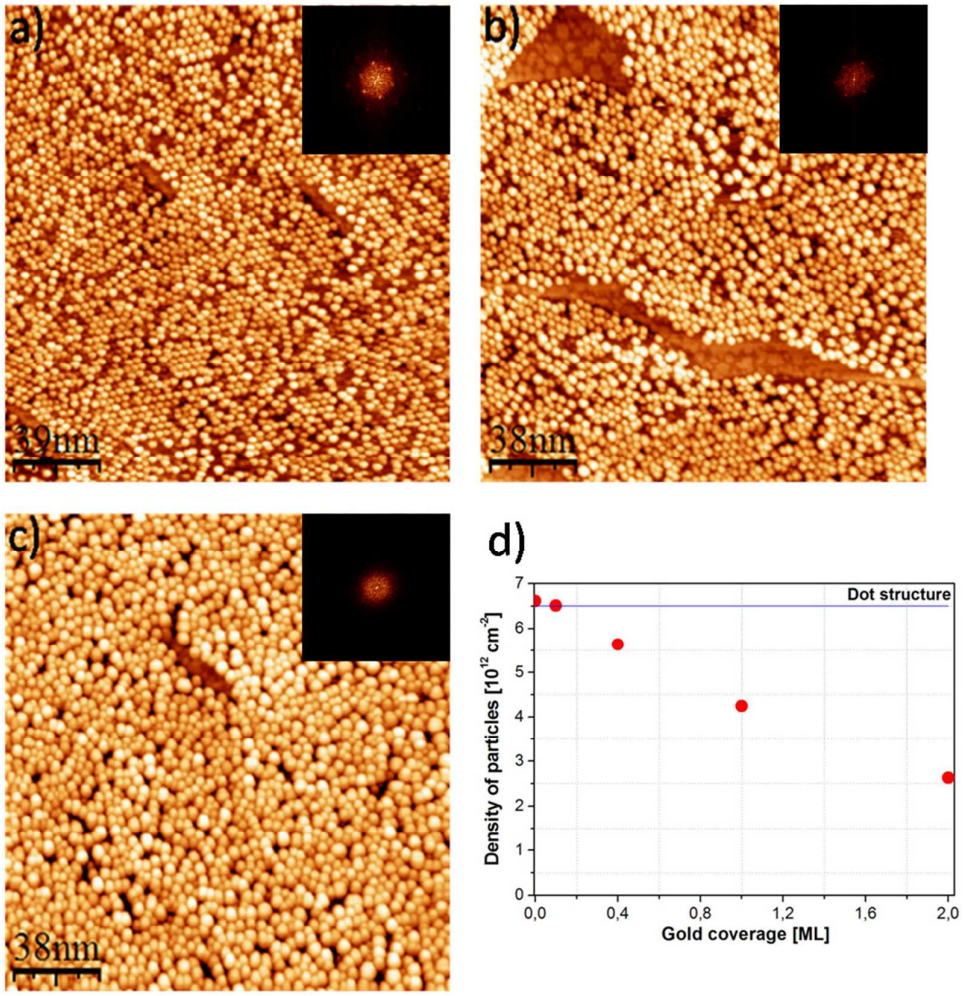

Figure 10: STM images (I_t = 19 pA, U= 1.51 V) corresponding to increasing amounts of Au deposited (a: 0.1 ML, b: 0.4 Ml, c: 1ML) on 0.4 ML of Pd. The insets are he Fourier transforms of the STM images. The density of clusters as a function of the amount of Au is plotted in (d). The mean size of the clusters is 117, 188, and 329 atoms for images (a), (b) and (c), respectively.

Figure 10 presents a series of STM images from increasing amount of Au deposited on 0.4 ML of Pd. Contrary to results presented on figure 9 we see that at 0.4 ML of gold disorder is present that increases with the amount of deposited Au. The apparition of disorders in the array of PdAu particles goes together with a reduction of the density of clusters which is a sign of mobility coalescence. It is noticeable that the coalescence occurs at a lower coverage for PdAu than for pure Pd (0.8 ML against

1.5 Ml). This could be interpreted by the presence of Au atoms at the interface that decreases the bonding of the cluster with the substrate. To clarify this point we have plotted the density of clusters as function of the total quantity of matter (figure 11a) and as a function of the percentage of Au contained in the clusters (figure 11b) for two series of experiments (0.15 Ml of predeposited Pd and 0.4 ML of predeposited Pd.

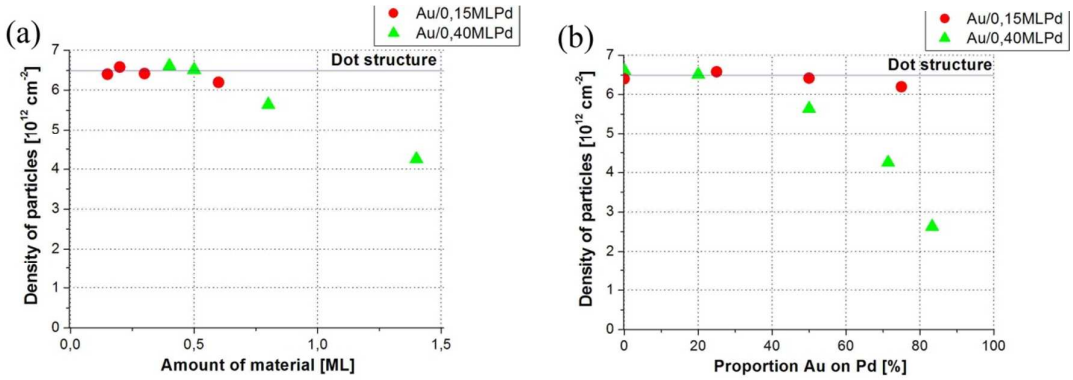

Figure 11: Variation of the density of clusters as a function of the total amount of deposited matter (a) and as a function of the concentration of Au in the clusters (b). The red and green points correspond to predeposition of 0.15 and 0.4 ML of Pd.

Figure 11 show that mobility coalescence is more related to the total coverage than to the concentration of Au in the clusters. Indeed coalescence appears at a total coverage of about 0.8 ML while in the case of 0.15 ML of predeposited Pd there is no coalescence even at a gold content of 80%. Thus the clusters become mobile when they reach a certain size and this critical size is smaller for PdAu clusters than for pure Pd clusters.

The long range order of the bimetallic particles has been characterized by GISAXS as for pure Pd [26]. Figure 12 displays three GISAXS patterns corresponding to 0.5 ML of Pd (a), 0.5 ML of Au deposited on the same sample (b) and after a total deposition of 1 ML of Au on the pure Pd sample (c). On the pure Pd (a) sharp peaks come from the clusters which are on the nodes of the dot structure. Contrary to STM the X-ray beam probe the whole sample, then we are sure that the array of Pd clusters is well organized on the whole sample. After the first deposition of gold the peaks are present but their intensity is increased proving that Au is only deposited on the array of Pd clusters. After the second deposition of gold the peaks have increased in width meaning that the size distribution is wider. However some intensity is present between the main GISAXS peaks and the central peaks it corresponds to clusters which are at larger distances between them. They results from dynamical coalescence events that are clearly present at this coverage from STM images (see figure 10).

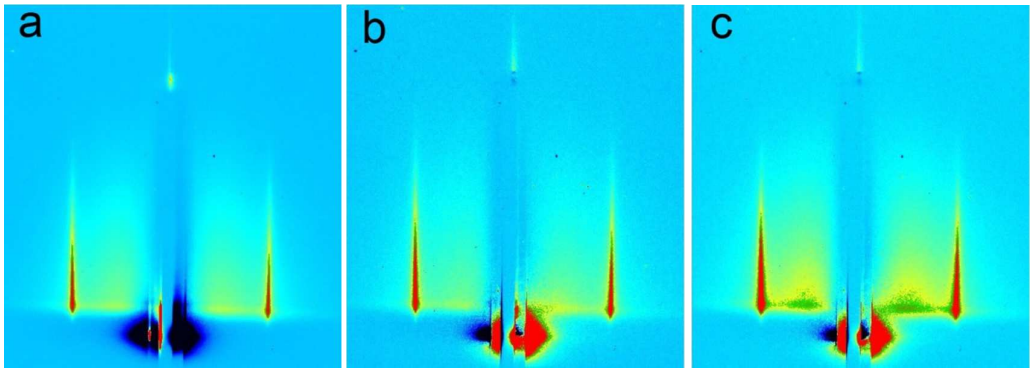

Figure 12: GISAXS patterns from 0.5 ML of Pd (a), 0.5 ML Pd + 0.5 ML Au (b) and 0.5 ML Pd + 1 ML Au (c)

As for pure Pd the thermal stability of the PdAu arrays has been checked by annealing at increasing temperatures. Figure 13 shows the evolution of the organization of the clusters as a function of the annealing temperature. Up to 600 K, as in the case of pure Pd, the PdAu clusters stay well ordered. From 630 K some disorder is present and at 670 K the density of clusters decreased strongly by coalescence. This behavior is similar to that has been observed on pure Pd. Figure 14 displays the evolution of the cluster number density of clusters as a function of annealing temperature which is similar for the two systems. However a difference between the two systems is visible in the STM pictures of PdAu arrays after annealing which already appears at 470 K (see figure 13). Some clusters appear brighter and higher than the others, contrary to the case of pure Pd where the cluster present about the same contrast and small variation of diameter. At 470 K the array of PdAu is still highly ordered, no coalescence has occurred. From the statistical analysis of the cluster height the average value has effectively decreased. We cannot interpret this observation by a loss of matter specific to PdAu because at this temperature Au cannot desorb from a silica film before 1100K [45] and no diffusion of Au atoms in the substrate has been observed at this temperature [46]. What can be changed by annealing of the PdAu clusters at 470 K? The PdAu clusters made 0.15 ML of each metal contain on the average 70 atoms. At this size more than half of the atoms are on the surface. After growth, all gold atoms are on top of the Pd predeposited cluster. Au is completely miscible in Pd but diffusion is limited at 320K. Thermodynamically Au as tendency to segregate on the surface [47, 48] but recent theoretical calculations have shown that the surface concentration of Au decreased with cluster size and also when temperature increases [49]. For a 50/50 composition a 55 atoms PdAu clusters the surface concentration of Au is 65 % at 300K while it is more than 95 % for bulk alloy. Therefore it is expected that by annealing the PdAu clusters Pd segregates on the surface of the clusters which was originally covered by gold. This change of surface composition could lead to a change of the height measured by STM. But it is also possible that the shape of the cluster evolves towards more stable structures upon annealing [50].

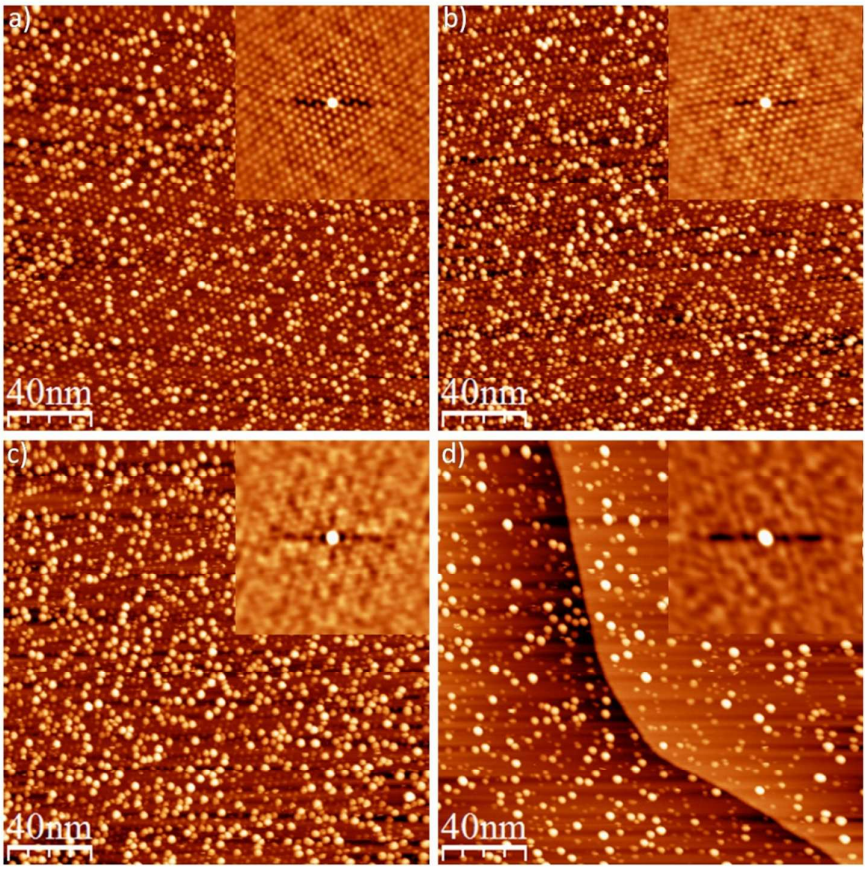

Figure 13: Evolution of an array of PdAu clusters made of 0.15 ML of Pd and 0.15 Ml of Au with the annealing temperature, (a) 470 K, (b) 590 K, (c) 630 K and (d) 670 K. The STM images are recorded at It = 19 pA and U = 1.49V. The insets represent self-correlation of the STM images.

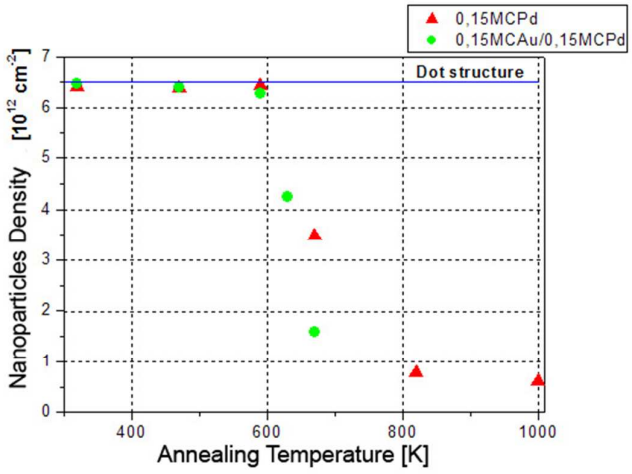

Figure 14: Evolution of the number density of Pd clusters (0.15 ML, red points) and PdAu clusters (0.15 ML Pd + 0.15 ML Au, green points) as a function of the annealing temperature.

5. **Discussion: Use of regular arrays of Pd and PdAu clusters as model catalysts**

Regular arrays of Pd and PdAu clusters have been prepared by growth from vapor under UHV at 320K on nanostructured alumina ultrathin films. In the case of pure Pd, hexagonal arrays of clusters with a high density ($6.5x10^{12}$ cm^{-2}) which is fixed by the nanostructure of the alumina film can be prepared in a large range of size from few atoms to about 400 atoms. The size dispersion is very narrow and follows a Poisson distribution [26, 44]. The array of clusters is perfectly ordered up to 1ML of Pd which corresponds to a size of 235 atoms. For thicker deposits the organization is less regular but the size distribution stays narrow. Growth coalescence occurs at 5 ML then the size distribution becomes wide and the clusters are no longer organized. The organization of the arrays of Pd clusters is preserved at high temperature until 600 K. At higher temperature clusters can escape from the nodes of the nanostructures and coalesce. These arrays of Pd are best suited model catalysts especially to study pure size effects. We have used such Pd arrays to study by a pulsed molecular beam technique the evolution of the adsorption energy of CO on the Pd clusters as a function of their size [26]. They could be used easily in important catalytic reaction like CO oxidation, hydrogenation unsaturated hydrocarbons. A major advantage of these arrays of clusters, compared to soft landed size selected clusters which can achieved atomically precise size selection (at least for clusters smaller than about one hundred atoms), is the unique possibility to study accurately the effect of the distance between neighboring clusters. The main effect is the reverse spillover which occurs when reactants adsorbed on the support diffuse toward the reactive clusters where they become adsorbed. The rate of adsorption depends on the size and on the distance between the clusters [51]. This phenomenon is important in adsorption kinetics [51, 52] but also in the kinetics of catalytic reactions when adsorption of one of the reactants is the rate limiting step [53]. If the clusters are regularly distributed in an array, the diffusion and the capture of reactant molecules can be exactly calculated [51], then the true effect of cluster size in the adsorption process can be investigated [53c].

Regular arrays of PdAu bimetallic clusters are prepared by depositing at 320 K Pd first then Au which grows only on the prenucleated Pd clusters. By this method the size and the composition of the bimetallic clusters are independently controlled. The PdAu clusters are well ordered in a hexagonal array which follows the dot structure of the nanostructured alumina film. The organization of the arrays is almost perfect up to a total coverage of 0.8 ML, corresponding to a cluster size of 188 atoms, independently of the proportion of gold. For larger clusters the size dispersion, although larger, remains narrow until about 5ML when static coalescence occurs. The organization of the PdAu clusters is stable upon annealing in UHV up to 600K as for pure Pd. The density of clusters is very high that provides a very high sensitivity in the reactivity studies even for few atoms clusters. By this method it is now possible to study the reactivity of bimetallic clusters of a large scale of size and to investigate for each size the whole range of composition. It is particularly interesting to study small sizes for which ab initio calculations can be undertaken. For pure monometallic free clusters ab initio calculations can be performed up to about 200 atoms [54]. But in the case of bimetallic clusters, many more configurations have to be considered. For PdAu clusters ab initio calculations have been performed up to a size close to 100 atoms [50, 55]. In addition in the case of tiny clusters it could become necessary to include in the calculation the ultrathin oxide film and the metal support underneath because charge transfer can occur between the metal support and the clusters through the thin oxide film [3, 56].

REFERENCES

[1] C.T. Campbell, Surf. Sci. Rep. ; 27(1997)1

[2] C.R. Henry, Surf. Sci. Rep., 31(1998)235

[3] H.J. Freund, M. Heyde, N. Nilius, S. Schauermann, S. Shaikhudtinov, M. Sterrer, J. Catal. 308(2013)154

[4] S.M. Mc. Clure, D.W. Goodman; Topics Catal. 54(2011)349

[5] C.R. Henry in 'Nanocatalysis' Eds. U. Heiz and U. Landman, Springer, Berlin (2007)245-268

[6] C.R. Henry, C. Becker in 'Surface Science and Interface Science' Vol. 4, Ed. K. Wandelt, Wiley-VCH (2014) P. 815-862

[7] A.S. Wörz, K. Judai, S. Abbet, U. Heiz; J. Am. Chem. Soc. 125(2003)7964

[8] M. Arenz, U. Landman, U. Heiz; ChemPhysChem 7(2006)1871

[9] W.E. Kaden, W.A. Kunkel, F.S. Roberts, M. Kane, S.L. Anderson; J. Chem. Phys. 136(2012)204705

[10] G. Kwon, G.A. Ferguson, C.J. Heard, E.C. Tyo, C. Yin, J. DeBartolo, S. Seifert, R.E. Winans, A.J. Kropf, J. Greeley, R.L. Johnston, L.A. Curtiss, M.J. Pellin, S. Vajda; ACS Nano7(2013)5807

[11] R. Alayan, L. Arnaud, M. Broyer, E. Cottencin, J. Lermé, S. Marhaba, J.L. Vialle, M. Pellarin; Phys. Rev. B 76(2007)075424

[12] R.E. Palmer, S. Pratontep, H-G. Boyen ; Nature Materials 2(2003)443

[13] H. Brune, M. Giovannini, K. Broman, K. Kern ; Nature 394(1998)451

[14] V. Repain, G. Baudot, H. Ellmer, S. Rousset; Europhys. Lett. 58(2002)730

[15] G. Prévot, H. Guesmi, B. Croset; Surf. Sci. 601(2007)2017

[16] C. Becker, K. von Bergmann, A. Rosenhahn, J. Schneider, K. Wandelt; Surf. Sci. 486(2001)L443

[17] T. Maroutian, S. Degen, C. Becker, K. Wandelt and R. Berndt; Phys. Rev. B 68(2003)155414

[18] G. Hamm, C. Barth, C. Becker, K. Wandelt, C.R. Henry; Phys. Rev. Lett. 97(2006)126106

[19] S. Gritschneder, C. Becker, K. Wandelt, M. Reichling; J. Am. Chem. Soc. 129(2007)4925

[20] M. Schmid, G. Kresse, A. Buchsbaum, S. Gritschneder, M. Reichling, P. Varga; Phys. Rev. Lett. 99(2007)196104

[21] A. Wiltner, A. Rosenhahn, J. Schneider, C. Becker, P. Pervan, M. Milun, M. Kralj, K. Wandelt; Thin Solid Films 400(2001)71

[22] C. Becker, A. Rosenhahn, A. Wiltner, K. von Bergmann, J. Schneider, P. Pervan, M. Milun, M. Kralj, K. Wandelt; New J. Phys. 4(2002)75

[23] M. Marsault, G. Hamm, A. Wörz, G. Sitja, C. Barth, C.R. Henry; Faraday Discuss. 138(2008)407

[24] S. Degen, C. Becker, K. Wandelt; Faraday Discuss. 125(2003)343

[25] G. Hamm, C. Becker, C.R. Henry; Nanotechnology 17(2006)1943

[26] G. Sitja, S. Le Moal, M. Marsault, G. Hamm, F. Leroy, C.R. Henry ; Nanolett. 13(2013)1977

[27]A. Lehnert, A. Krupski, S. Degen, K. Franke, . Decker, S. Rusponi, M. Kralj, C. Becker, H. Brune, K. Wandelt; Surf. Sci. 600(2006)1804

[28] A. Buchsbaum, M. De Santis, H.C.N. Talentino, M. Schmid, P. Varga ; Phys. Rev. B 81(2010)115420

[29] C.R. Henry and C. Barth in 'Nanoalloys, Synthesis, Structure and Properties', Eds. D. alloyeau, C. Mottet, C. Ricolleau, Springer (2012) p. 25-68

[30] L. Gragnaniello, T. Ma, G. Barcaro, L. Semanta, F.R. Negreiros, A. Fortunelli, S. Surnev, F.P. Netzer ; Phys. Rev. Lett. 108(2012)195507

[31] M. Heemeir, A.F. Carlsson, M. Naschitzki, M. Schmal, M. Bäumer, H-J. Freund; Angew. Chem. Int. Ed. 41(2002)4073

[32] G. Sitja, M. Marsault, F. Leroy, S. La Moal, C.R. Henry ; Int. J. Technol. 9(2012)567

[33] G. Renaud, R. Lazzari, C. Revenant, A. Barbier, M. Noblet, O. Ullrich, F. Leroy, Y. Borensztein, J. Jupille, C.R. Henry, J. P. Deville, F. Scheurer, J. Mane-Mane, O. Fruchart ; Science 300(2003)1416

[34] A.T. N'Diaye, S. Bleikamp, P.J. Feibelman, T. Michely ; Phys. Rev Lett. 97(2006)215501

[35] K. Donner, P. Jakob; J. Chem. Phys. 131(2009)164701

[36] M. Sicot, S. Bouvron, O. Zander, U. Rüdiger, Yu.S. Dedkov, M. Fonin; Appl. Phys. Lett. 96(2010)093115

[37] Q. Liao, H.J. Zhang, H.Y. Li, S.N. Bao, P. He; Nanotechnology 22(2011)125503

[38] Z. Zhou, F. Gao, D.W. Goodman; Surf. Sci. 604(2010)L31

[39] J. Zhang, V. Sessi, C.H. Michaelis, I. Brihuega, J. Honolka, K. Kern ; Phys. Rev. B 78(2008)165430

[40] T. Gerber, J . Knudsen, P.J. Feibelman, E. Granäs, P. Stratmann, K. Schulte, J.N. Andersen, T. Michely; ACS Nano 7(2013)2020

[41] X. Xu, J. Szanyi, Q. Xu, D.W. Goodman; Catal. Today 21(1994)57

[42] K. Hojrup Hansen, T. Worren, S. Stemple, E. Laegsgaard, M. Bäumer, H-J. Freund, F. Besenbacher, I. Stensgaard; Phys. Rev. Lett. 83(1999)4120

[43] E. Napetschnig, M. Schmid, P. Varga; Surf. Sci. 601(2007)3233

[44] G. Sitja, R. Omar Unac, C.R. Henry; Surf. Sci. 604(2010)404

[45] C.C. Chusuei, X. Lai, K. Luo, D.W. Goodman ; Topics in Catal. 14(2001)71

[46] M. Marsault, PhD Thesis, Université de la Méditerranée (Marseille) 2010

[47] K. Luo, T. Wei, C.W. Yi, S. Axnanda, D.W. Goodman; J. Phys. Chem. B 109(2005)23517

[48] A.R. Haire, J. Gustafson, A.C. Trant, T.E. Jones, T.C.Q . Noakes, P. Bailey, C.J. Baddeley; Surf. Sci. 605(2011)214

[49] B. Shan, L. Wang, S. Yang, J. Hyun, N. Kapur, Y. Zhao, J.B. Nicholas, K. Cho; Phys. Rev. B 80(2009)035404

[50] F. Pittaway, L.O. Paz-Borbon, R.L. Johnston, H. Arslan, R. Ferrando, C. Mottet, G. Barcaro, A. Fortunelli; J. Phys. Chem C 113(2009)9141

[51] C.R. Henry, C. Chapon, C. Duriez; J. Chem. Phys. 95(1991)700

[52] (a) E. Gillet, S. Channakhone, V. Matolin, J. Catal. 97(1986)437 , (b) L. Piccolo, C.R. Henry, Surf. Sci. 452(2000)198

[53] (a) S. Ladas, H. Poppa, M. Boudart, Surf. Sci. 102(1981)151; (b) C.R. Henry Surf. Sci. 223(1989)519, (c) L. Piccolo, C.R. Henry, J. Mol. Cat. A167(2001)181; (d) J. Libuda, H.J. Freund, Surf. Sci. Rep.57(2005)157, (e) M. Röttgen, S. Abbet, K. Judai, J-M. Antonietti, A.S. Wörz, M. Arenz, C.R. Henry, U. Heiz, J. Am. Chem. Soc. 129(2007)9635

[54] (a) U. Landman, B. Yoon, C. Zhang, U. Heiz, M. Arenz; Top. Catal. 44(2007)145; (b) C. Mager-Maury, G. Bonnard, C. Chizallet, P. Sautet, P. Raybaud, ChemCatChem 3 (2011)200 ; (c) A. D. Allian, K. Takanabe, K. L. Fujdala, X. Hao, T. J. Truex, J. Cai, C. Buda, M. Neurock, E. Iglesia, J. Am. Chem. Soc., 133 (2011) 4498; (d) I.V. Yudanov, A. Genest, S. Schauermann, H.J. Freund, N. Rösch; Nano Lett. 12(2012)2134; (e)G. Allen Ferguson, F. Mehmood, R.B. Rankin, J.P. Greeley, S. Vajda, L.A. Curtiss Top. Catal. 55(2012)353

[55] (a) D. Yuan, X. Gong, R. Wu; Phys. Rev. B 78(2008)035441; (b) I. Y. Yudanov, K. M. Neyman; PCCP 12(2010)5094; (c) B. Zhu, G. Thrimurthulu, L. Delannoy, C. Louis, C. Mottet, J. Creuze, B. Legrand, H. Guesmi, J. Catal. 308 (2013)272

[56] L. Giordano, G. Pacchioni, J. Goniakowski, N. Nilius, E.D.L. Rienks, H-J. Freund, Phys. Rev. Lett. 101(2008)026102